

Preyssler catalyst: An efficient catalyst for esterification of cinnamic acids with phenols and imidoalcohols

Diego M. Ruiz^{a,*}, Gustavo P. Romanelli^{a,b}, Patricia G. Vázquez^b, Juan C. Autino^a

^a Cátedra de Química Orgánica, Facultad de Ciencias Agrarias y Forestales, UNLP, Calles 60 y 119, (B1904AAN) La Plata, Argentina

^b Centro de Investigación y Desarrollo en Ciencias Aplicadas “Dr. Jorge J. Ronco” (CINDECA), Departamento de Química, Facultad de Ciencias Exactas, UNLP-CCT-CONICET, Calle 47 N° 257, (B1900AJK) La Plata, Argentina

ARTICLE INFO

Article history:

Received 3 September 2009

Received in revised form 21 November 2009

Accepted 25 November 2009

Available online 1 December 2009

Keywords:

Acid catalysis

Cinnamates

Esterification

Heteropolyacid

Preyssler heteropolyacids

ABSTRACT

In the present work a series of eco-friendly Preyssler solid acids and their salts $H_{14}[NaP_5W_{29}MoO_{110}]$ (PW), $H_{14}[NaP_5W_{30}O_{110}]$ (PWMo), $K_{12.5}Na_{1.5}[NaP_5W_{30}O_{110}] \cdot 15H_2O$ (PWK), $K_{12.5}Na_{1.5}[NaP_5W_{29}MoO_{110}] \cdot 15H_2O$ (PWMoK) and 10% silica-supported $H_{14}[NaP_5W_{29}MoO_{110}]$ (PWSiO₂), and $H_{14}[NaP_5W_{30}O_{110}]$ (PWMoSiO₂) have been used as catalysts for the direct esterification of cinnamic acids with phenols or 2-(N-phthalimidoethanol). Effects of the reaction conditions were studied, including temperature, reaction time, and type and amount of catalyst. These solids were characterized by several techniques, such as diffuse reflectance spectroscopy, Fourier transformed infrared spectroscopy, optical and scanning electron microcopies, and X-ray diffraction, among others.

The most adequate catalyst for performing the title reaction was $H_{14}[NaP_5W_{30}O_{110}]$ (PWMo). The catalyst was applied for the synthesis of various substituted cinnamates, giving very good yields.

© 2009 Elsevier B.V. All rights reserved.

1. Introduction

Catalysis by heteropolyacids (HPAs) and related compounds is a field of increasing importance worldwide. Numerous developments are being carried out in basic research as well as in fine chemistry processes [1]. HPAs possess, on the one hand, a very strong acidity and, on the other hand, appropriate redox properties, which can be changed by varying the chemical composition of the heteropolyanion. The reactions catalyzed by both heterogeneous and homogeneous systems have been reviewed by many researchers [2–10].

The reactions in which they can be used, from dehydration, cyclization or esterification up to amine oxidation or olefin epoxidation, may find wide applications in fine chemical production, such as fragrances, pharmaceuticals and food [11,12].

Although there are many structural types of HPAs, the majority of catalytic applications use the most common Keggin type [13], especially for acid catalysts, owing to its availability and chemical stability. Other catalysts such as Wells-Dawson and Preyssler heteropolyacids have begun to be used. [14–16].

The Preyssler heteropolyanion consists of a cyclic assembly of five PW_6O_{22} units, each derived from the Keggin anion $[PW_{12}O_{40}]^{3-}$ by the removal of two sets of three corner-sharing WO_6 octahedra. A sodium ion is located within the polyanion on the five-fold axis and 1.25 Å above the pseudo mirror plane that contains the five phosphorus atoms. This heteropolyanion with 14 acidic protons is an efficient superacid solid catalyst that can be used both in homogeneous and heterogeneous phases. Preyssler catalyst is a green catalyst with respect to safety, noncorrosive properties, quantity of waste separability, and stability [17].

Recent applications related to the catalytic activity of the Preyssler heteropolyoxometalates in organic synthesis include esterification of n-butanol with acetic acid [18], alkylation of phenol with 1-octene [19], synthesis of isoxazoles [20], coumarins [13], 2,4,6-triarylpyridines [21], 2-amino-4H-chromenes [22], and 1,5-benzodiazepine [23], and oxidation reactions such as alcohols [24], primary aromatic amines [25] and thiols using air as oxidant [26], and alkene epoxidation [27].

On the other hand, α,β -unsaturated esters possess various pharmacological activities including antioxidant, antimicrobial and anticancer activities [28], besides being useful in other synthetic applications. There are numerous methods for the preparation of α,β -unsaturated esters; however, most of the reported procedures require strong acids such as sulfuric acid, hydrochloric acid and toxic chemicals such as dimethyl sulfate, methyl iodide or diazomethane, which are environmentally

* Corresponding author at: Cátedra de Química Orgánica, Departamento de Ciencias Exactas, Facultad de Ciencias Agrarias y Forestales UNLP, Calle 60 y 119 S/N, (B1904AAN) La Plata, Argentina.

E-mail address: dimruiz@agro.unlp.edu.ar (D.M. Ruiz).

hazardous and hence unacceptable [29]. Particularly, cinnamates are enormously important organic compounds due to their application in a wide range of industrial products such as plasticizers, graphics, lubricants, flavors, perfumes and cosmetics [29]. Cinnamates are also antioxidant and flavoring agents in diverse plant species. A bioactive imidoalkyl cinnamate, 2-(N-phthalimido) ethyl cinnamate, is a potent inhibitor of the 17- β -hydroxysteroid dehydrogenase enzyme related to diseases such as breast cancer, Alzheimer disease and benign prostatic hyperplasia [30]. Aryl cinnamates have been used as intermediates for diverse heterocyclic compounds, such as chromones, pyrazoles and furanones [31]. Some substituted aryl cinnamates are plant-growth inhibitors [32] and have antifungal [30] activity.

Only a few procedures have been used to prepare aryl cinnamates, including the most used method via cinnamoyl chloride [33], the use of DCC [34] or BOP [30] as coupling agents to perform the direct reaction between cinnamic acid and phenol, or from phosphorane and benzaldehyde [35]. Most recently our research group described a green procedure to prepare these compounds for the direct esterification of cinnamic acids with phenols or 2-(N-phthalimido)ethanol using a Wells-Dawson heteropolyacid bulk or supported on silica [36]. Under environmentally friendly conditions, other cinnamates have been obtained from cinnamaldehydes using a heterogeneous catalyst and DDQ [37], and direct esterification using water-tolerant $\text{ZrOCl}_2 \cdot 8\text{H}_2\text{O}$ and $\text{HfOCl}_2 \cdot 8\text{H}_2\text{O}$ as catalysts [29].

In connection with our research project on the eco-friendly synthesis of organic compounds related to selective pesticides, we report the results obtained for the direct esterification between cinnamic acids (**1**) and phenols (**2b**) or 2-(N-phthalimido)ethanol (**2a**) (Scheme 1). A series of solid acids or salts with Preyssler structure, such as $\text{H}_{14}[\text{NaP}_5\text{W}_{29}\text{MoO}_{110}]$ (PW), $\text{H}_{14}[\text{NaP}_5\text{W}_{30}\text{O}_{110}]$ (PWMo), $\text{K}_{12.5}\text{Na}_{1.5}[\text{NaP}_5\text{W}_{30}\text{O}_{110}] \cdot 15\text{H}_2\text{O}$ (PWK), $\text{K}_{12.5}\text{Na}_{1.5}[\text{NaP}_5\text{W}_{29}\text{MoO}_{110}] \cdot 15\text{H}_2\text{O}$ (PWMoK) and 10% silica-supported $\text{H}_{14}[\text{NaP}_5\text{W}_{29}\text{MoO}_{110}]$ (PWSiO₂), and $\text{H}_{14}[\text{NaP}_5\text{W}_{30}\text{O}_{110}]$ (PWMoSiO₂), were employed as eco-friendly and reusable catalysts in bulk and silica-supported form; in both cases heterogeneous catalysis takes place.

2. Materials and methodology

2.1. Catalyst preparation

2.1.1. Bulk catalysts

The Preyssler salt, $\text{K}_{12.5}\text{Na}_{1.5}[\text{NaP}_5\text{W}_{30}\text{O}_{110}] \cdot 15\text{H}_2\text{O}$ (PWK), was prepared from $\text{Na}_2\text{WO}_4 \cdot 2\text{H}_2\text{O}$ according to a previously reported method [38] and converted to the corresponding acid $\text{H}_{14}[\text{NaP}_5\text{W}_{29}\text{MoO}_{110}]$ (PW), by passing it through a Dowex-50W-x8 ion-exchange column. For the preparation of the Mo-substituted Preyssler salt $\text{K}_{12.5}\text{Na}_{1.5}[\text{NaP}_5\text{W}_{29}\text{MoO}_{110}] \cdot 15\text{H}_2\text{O}$ (PWMoK), a procedure similar to the preparation of PWK was adapted and described in the literature [39]. In a typical

experiment 56 g (0.169 mol) $\text{Na}_2\text{WO}_4 \cdot 2\text{H}_2\text{O}$ and 2 g (0.008 mol) $\text{Na}_2\text{MoO}_4 \cdot 2\text{H}_2\text{O}$ were dissolved in 70 ml water and mixed at 60 °C for 30 min. The solution was cooled to room temperature and 45 ml concentrated phosphoric acid was added. The resulting yellow solution was refluxed for 18 h. The color turned to dark green at the end of reaction. The solution was brought to room temperature, diluted with 30 ml water and then 20 g potassium chloride was added with stirring. The mixture was stirred for 30 min and then heated up to dryness, and a greenish solid was obtained. This raw product was dissolved in 70 ml warm water and upon cooling to room temperature yellow crystals formed, which were collected and recrystallized from boiling water (yield, 18%). The Mo-substituted heteropolyanion was converted to its corresponding acid $\text{H}_{14}[\text{NaP}_5\text{W}_{29}\text{MoO}_{110}]$ (PWMo), by passing an aqueous solution of PWMoK through a Dowex-50W-x8 ion-exchange column.

2.1.2. Supported catalysts

Silica gel-supported Preyssler acids were prepared by wet impregnation of Grace silica (SiO_2) (Grade 59, specific area: 250 m²/g), with an acetone solution of PW or PWMo synthesized heteropolyacids, respectively. Then, two supported catalysts, PWSiO₂, and PWMoSiO₂, containing 10 wt% of active phase, were prepared. After impregnation, samples were dried at room temperature in vacuum desiccators for 8 h.

2.2. Catalyst characterization

2.2.1. Textural analysis

The specific surface area (SBET) of supports and catalysts was determined by nitrogen adsorption/desorption techniques using Micromeritics Accusorb 2100E equipment.

2.2.2. Diffuse reflectance spectroscopy (DRS)

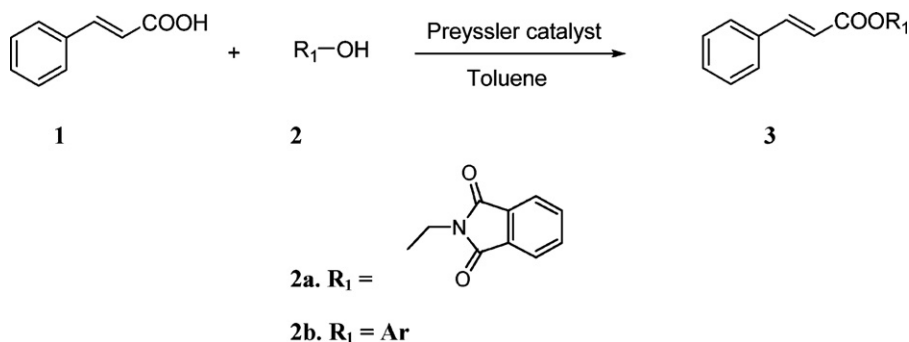
The solid samples were studied in the range 200–600 nm, using UV–vis Varian Super Scan 3 equipment, fitted with a diffuse reflectance chamber with an inner surface of BaSO₄. Samples were compacted in a Teflon sample holder to obtain a sample thickness of 2 mm.

2.2.3. Fourier transformed infrared spectroscopy (FT-IR)

Bruker IFS 66 equipment, pellets with KBr, and a measuring range of 400–1500 cm⁻¹ were used to obtain the FT-IR spectra of the solid samples.

2.2.4. X-ray diffraction (XRD)

XRD patterns of representative solid samples were recorded by means of a Philips PW-1732 device with built-in recorder, using the following conditions: Cu K α radiation; Ni filter; 30 mA and 40 kV in the high voltage source; scanning angle (2 θ) from 5° to 50° and scanning rate, 1° min⁻¹.



Scheme 1.

2.2.5. SEM analysis

The catalysts were characterized with a Philips 505 scanning electron microscope (SEM) using an accelerating voltage of 15 eV. The samples were fixed as powder on a graphitized band and coated with graphite.

2.2.6. Acidity measurements

An amount of 0.05 ml of 0.1N n-butylamine (Carlo Erba) in acetonitrile (J.T. Baker) was added to a known mass of solid (0.05 g for bulk and 0.4 g for supported solids) using acetonitrile as solvent, and stirred for 3 h. Later, the suspension was titrated with the same base at 0.05 ml/min. The electrode potential variation was measured with an Instrumentalia S.R.L. digital pHmeter, using an LL Solvotrode LiCl–ethanol electrode. The acidic properties of the samples measured by this technique enable the evaluation of the number of acid sites and their acid strength. In order to interpret the results, it is suggested that the initial electrode potential (E) indicates the maximum acid strength of the surface sites, and the values (meq/g solid), where the plateau is reached, indicate the total number of acid sites. The acid strength of surface sites can be assigned according to the following ranges: very strong site, $E > 100$ mV, strong site, $0 < E < 100$ mV; weak site, $-100 < E < 0$ mV, and very weak site, $E < -100$ mV.

2.3. General procedures and statements

All the reactions were monitored by TLC on precoated silica gel plates (254 μ m). Flash column chromatography was performed with 230–400 mesh silica gel. All the yields were calculated from crystallized products. All the products were identified by comparison of physical data (mp, TLC, NMR) with those reported or with those of authentic samples prepared by the respective conventional methods using sulfuric acid as catalyst. Melting points of the compounds were determined in sealed capillary tubes and are uncorrected. ^{13}C NMR and ^1H NMR spectra were recorded at room temperature on Bruker AC-250 and Bruker Advance DPX-400 spectrometers using TMS as internal standard. Entries and target compounds have the same number.

2.4. Catalytic test

All catalysts were dried overnight prior to use. The esterification reaction was performed in a round bottom flask, which was equipped with a condenser and immersed in an oil bath. A solution of cinnamic acid **1** (1.1 mmol) and 2-phthalimidoethanol **2a** or phenol **2b** (1 mmol) in toluene (4 ml) and the bulk or silica-supported WD acid (10–2 mmol) were refluxed with stirring for the indicated time. In both cases the catalyst was removed by filtration and washed twice with toluene (1 ml each). The organic solution was washed with cold 1 M NaOH (2×2 ml) and H_2O (2×2 ml) and then dried over anhydrous Na_2SO_4 . Evaporation of the solvent under reduced pressure and recrystallization from petroleum ether, or silica flash column chromatography gave the pure cinnamate **3**.

2.5. Spectral data for products

2.5.1. 2-Phthalimidoethyl cinnamate

Colorless solid, mp 114–115 °C (Lit. [40] 113–115 °C); ^1H NMR (400 MHz, CDCl_3): 3.01 (2H, t, $J = 7.3$ Hz), 4.50 (2H, t, $J = 7.2$ Hz), 6.37 (1H, d, $J = 15.8$ Hz), 7.30–7.58 (5H, m), 7.58–7.90 (4H, m), 7.59–7.61 (2H, m), 7.90 (1H, d, $J = 16$ Hz); ^{13}C NMR (100 MHz, CDCl_3): 37.2, 67.7, 105.6, 117.6, 123.4, 128.4, 129.1, 130.4, 130.6, 132.2, 134.3, 145.7, 166.9, 168.3.

2.5.2. 2-Phthalimidoethyl 3,4,5-trimethoxycinnamate

Colorless solid, mp 117–118 °C (Lit. [40] 118–120 °C); ^1H NMR (400 MHz, CDCl_3): 3.01 (2H, t, $J = 7.3$ Hz), 3.54 (9H, br s), 4.51 (2H, t, $J = 7.3$ Hz), 6.64 (1H, d, $J = 16$ Hz), 7.26–7.29 (2H, m), 7.43–7.81 (4H, m), 7.60 (2H, m), 7.90 (1H, d, $J = 16$ Hz); ^{13}C NMR (100 MHz, CDCl_3): 37.4, 56.4, 67.6, 105.6, 116.9, 123.4, 130.0, 132.2, 132.3, 134.0, 145.7, 153.6, 167.0, 168.4.

2.5.3. 2-Phthalimidoethyl 4-methylcinnamate

Colorless solid, mp 117–118 °C (Lit. no data); ^1H NMR (400 MHz, CDCl_3): 1.24 (3H, s), 3.01 (2H, t, $J = 7$ Hz), 4.50 (2H, t, $J = 7$), 6.64 (1H, d, $J = 16$ Hz), 7.26–7.29 (2H, m), 7.50–7.89 (4H, m), 8.04 (2H, d, $J = 16$ Hz); ^{13}C NMR (100 MHz, CDCl_3): 22.0, 37.2, 67.7, 116.2, 125.2, 128.4, 129.1, 129.5, 130.6, 132.2, 133.8, 148.0, 164.3, 168.3.

2.5.4. 2-Phthalimidoethyl 3-chlorocinnamate

Oil (Lit. no data); ^1H RMN (400 MHz, CDCl_3): 3.01 (2H, t, $J = 7$ Hz), 4.50 (2H, t, $J = 7$), 6.64 (1H, d, $J = 16$ Hz), 7.13–7.30 (4H, m), 7.59–7.61 (2H, m), 7.68–7.98 (4H, m), 8.04 (1H, d, $J = 16$ Hz); ^{13}C RMN (100 MHz, CDCl_3): 37.2, 67.7, 116.2, 124.9, 126.2, 127.4, 128.3, 129.1, 129.5, 129.8, 130.6, 131.9, 132.2, 135.8, 148.0, 164.3, 168.3.

2.5.5. Phenyl cinnamate

Colorless solid, mp 75–75.5 °C (Lit. [30] 75–76 °C); ^1H NMR (400 MHz, CDCl_3): 6.64 (1H, d, $J = 16$ Hz), 7.18 (2H, d, $J = 7.5$ Hz), 7.25 (1H, t, $J = 7.3$ Hz), 7.38–7.46 (5H, m), 7.56–7.62 (2H, m), 7.88 (1H, d, $J = 16$ Hz); ^{13}C NMR (100 MHz, CDCl_3): 117.4, 121.6, 125.8, 128.3, 129.0, 129.4, 130.7, 134.2, 146.6, 150.8, 165.4.

2.5.6. 4-Methylphenyl cinnamate

Colorless solid, mp 96–97 °C (Lit. [41] 97–97.5 °C); ^1H NMR (400 MHz, CDCl_3): 2.36 (3H, s), 6.62 (1H, d, $J = 16$ Hz), 7.04–7.06 (2H, m), 7.19–7.21 (2H, d, $J = 8.1$ Hz), 7.41–7.42 (3H, m), 7.57–7.59 (2H, m), 7.86 (1H, d, $J = 16$ Hz); ^{13}C NMR (100 MHz, CDCl_3): 20.9, 117.4, 121.3, 128.3, 129.0, 130.0, 130.6, 134.2, 135.4, 146.4, 148.6, 165.6.

2.5.7. 4-Methoxyphenyl cinnamate

Colorless solid, mp 99–101 °C (Lit. [42] 100–102 °C); ^1H NMR (400 MHz, CDCl_3): 3.74 (3H, s), 6.55 (1H, d, $J = 16$ Hz), 6.81–6.87 (2H, m), 6.99–7.05 (2H, m), 7.32–7.38 (3H, m), 7.48–7.54 (2H, m), 7.78 (1H, d, $J = 16$ Hz); ^{13}C NMR (100 MHz, CDCl_3): 55.6, 114.5, 117.4, 122.4, 128.3, 129.0, 130.6, 134.2, 144.3, 146.4, 157.3, 165.8.

2.5.8. 4-Bromophenyl cinnamate

Colorless solid, mp 111–112 °C (Lit. [43] 113–115 °C); ^1H NMR (400 MHz, CDCl_3): 6.60 (1H, d, $J = 16$ Hz), 7.06 (2H, d, $J = 8.9$ Hz), 7.25–7.38 (3H, m), 7.43 (2H, d, $J = 8.8$ Hz), 7.57–7.62 (2H, m), 7.86 (1H, d, $J = 16$ Hz); ^{13}C RMN (100 MHz, CDCl_3): 117.1, 119.1, 123.7, 128.6, 129.3, 131.1, 132.7, 134.3, 147.3, 150.1, 165.3.

2.5.9. 4-Nitrophenyl cinnamate

Colorless solid, mp 145–146 °C (Lit. [44] 145–146 °C); ^1H NMR (400 MHz, CDCl_3): 6.63 (1H, d, $J = 16$ Hz), 7.37 (2H, d, $J = 9$ Hz), 7.40–7.50 (3H, m), 7.55–7.65 (2H, m), 7.92 (1H, d, $J = 16$ Hz), 8.30 (2H, d, $J = 8$ Hz); ^{13}C NMR (100 MHz, CDCl_3): 116.2, 122.5, 125.2, 128.5, 129.1, 129.5, 133.8, 148.0, 155.6, 164.3.

2.5.10. 1-Naphthyl cinnamate

Colorless solid, mp 106–107 °C (Lit. [40] 105–108 °C); ^1H RMN (400 MHz, CDCl_3): 6.64 (1H, d, $J = 16$ Hz), 7.26–7.29 (2H,

m), 7.45–7.43 (3H, m), 7.59–7.61 (2H, m), 7.90 (1H, d, $J = 16$ Hz), 8.04 (2H, d, $J = 8.7$ Hz); ^{13}C RMN (100 MHz, CDCl_3), δ (ppm): 117.0, 118.1, 121.3, 125.4, 126.0, 126.4, 127.0, 128.0, 128.4, 129.0, 130.8, 134.2, 134.7, 146.7, 147.0, 165.4.

3. Results and discussion

3.1. Catalyst characterization

According to the literature [39], the characteristic bands associated with the Pope–Jeannin–Preyssler (PW) structure are three bands due to P–O stretching at 1163, 1079 and 1022 cm^{-1} , and two bands attributed to W–O–W at 941 and 913 cm^{-1} ; a band at 757 cm^{-1} corresponding to W=O; and one band at 536 cm^{-1} due to P–O bending. Finally, the H_2O bending at 1616 cm^{-1} is observed. The PWMo-substituted acid shows similar bands with little displacement. Previously, our investigations discussed the vibrational spectra of other heteropolycompounds (Keggin HPA) [45] as a function of the nature of the metal (Me) introduced, considered as a perturbing element. The typical spectrum is modified as follows: the introduction of a Me, other than W, in the structure (Mo in this case) induces a decrease of the W–O stretching frequencies and a possible splitting of the P–O band, depending on the Me nature. This splitting can be considered as an indirect evaluation of the strength of the Me–O interaction.

The spectra of silica, PW and PWMo supported on silica are shown in Fig. 1. As reported in the literature [11], silica exhibits three main bands at 1100, 800 and 470 cm^{-1} . The PW or PWMo band placed in the 1100 cm^{-1} region of the PW or PWMo on SiO_2 spectrum is masked by that of silica. Anyway, information can still be obtained from the less affected regions that show the characteristic bands that confirm the presence of the undegraded anion. These bands are those mentioned previously: 941 and 913 cm^{-1} (attributed to W–O–W), 757 cm^{-1} (corresponding to W=O), and finally, 536 cm^{-1} due to P–O bending.

X-ray diffraction patterns shown in Fig. 2 are similar with Preyssler structures, showing two main diffraction lines placed at 6.5° and 17.5° 2θ , and some wide, low intensity signals at 8.8° , 12° , 13.6° , 25.5° and 33.7° 2θ . All diffractograms shown in Fig. 2 present very low definition due to the experimental conditions used and to their high hygroscopicity during their scanning.

The information about the substitution of ions into the geometry of the structure is given by DRS spectra; the charge-transfer absorption spectra of the most nonreduced polyanions appear in the 200–500 nm region, and consist of bands attributed to oxygen–metal transfers [46]. The DRS spectra of PW, PWK and PWMoK are shown in Fig. 3. The PW acid presents two bands at 330

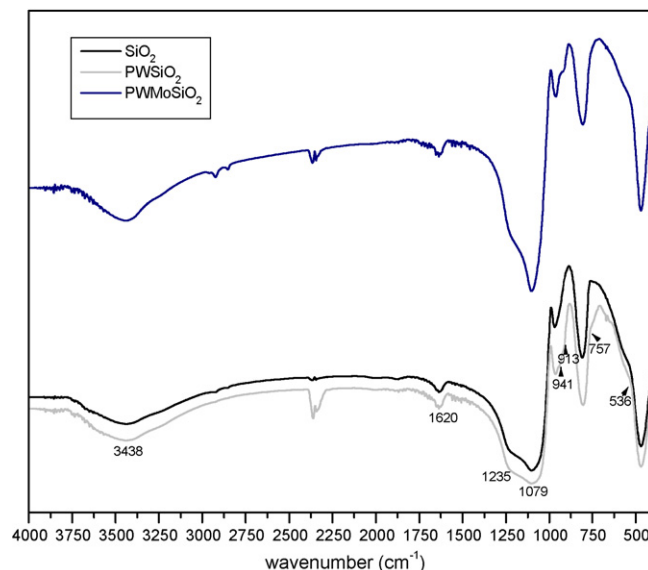


Fig. 1. FTIR spectra of silica and supported PW and PWMo.

and 380 nm; this result discards the structures of the main impurities from the synthesis of Preyssler acids, Wells–Dawson $\text{H}_6\text{P}_2\text{W}_{18}\text{O}_{62}$ (DRS bands at 190, 250 and 300 nm) and Keggin $\text{H}_3\text{PW}_{12}\text{O}_{40}$ (DRS bands at 190 and 260 nm) acids [47]. When PWK spectrum is observed, the second band is obtained at 340 nm, very close to the first one, and very different from the band at 380 nm when K is no present in the Pressley structure. PWMoK shows absorption bands at 310 and 330 nm shifted with respect to the characteristic bands at 220 and 260 nm of tetrahedral Mo, bands attributed to oxygen–metal transfers at 210–230 nm, and another one that extends up to 400 nm indicating Mo in octahedral position. These bands are present in the Keggin structure. This spectrum is difficult to be assigned an intact Preyssler structure, but with other techniques it is possible to say that the majority of the Pressley structure is present in the salt.

In relation to acidic properties, when measuring the strength of a solid acid or base, it should be recognized that activity coefficients for species on the solid are unknown. Acidity and basicity functions for the solid are not properly defined thermodynamically. The acid strength of a solid is defined as the ability of the surface to convert an adsorbed neutral base into its conjugated acid. In the case of the HPA studied it is not easy to analyze this property, so we will try to explain its behavior by potentiometric titration.

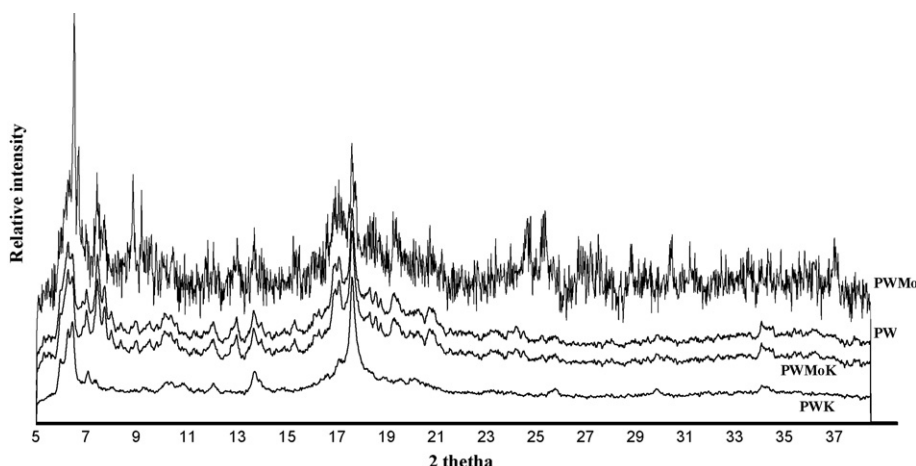


Fig. 2. XRD pattern for the acids and salts with Preyssler structure.

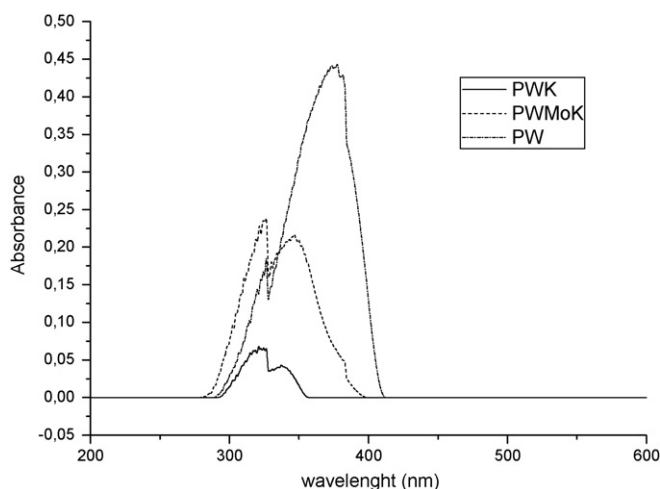


Fig. 3. DRS of acids and salts with Preyssler structure.

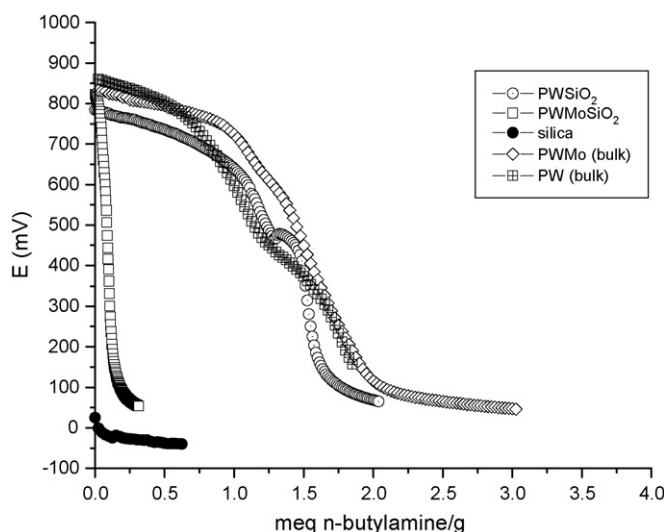


Fig. 4. Potentiometric titration curves of acids and salts with Preyssler structure.

The maximum acid strength of the acid sites for PW and PWMo is 862 and 833 mV, respectively (Fig. 3). This *E* indicates very strong acid sites for both bulk solid acids, very similar to the bulk Keggin HPA. The values of meq base/g solid where the plateau is reached indicate the total number of acid sites (11 for PW and 13 for PWMo). PWMoK shows weak acid sites (87 mV) and PWK gives a very weak maximum strength (−20 mV), not shown in this work.

As regards supported acids, the results show a low decrease in the maximum acid strength, 784 mV for PWSiO₂ (from 862 mV) and 822 mV for PWMoSiO₂ (from 833 mV). The support (silica) acid strength was tested, with an initial potential of 25 mV. When PW is supported on silica, the number of acid sites is very similar to bulk PW (Fig. 4). When Mo is incorporated into the structure of PW and then supported on silica, the initial *E* is very close to that of

bulk HPA, but the number of acid sites is different. From 822 mV, the potentiometric curve abruptly decreases to 50 mV for 0.3 meq of *n*-butylamine/g of catalyst. This behavior could be due to the fact that Mo presence could be inducing the redox internal reaction and the electron ring in the Preyssler structure could be stimulating it. In this case, the acidic properties decrease.

In relation to the textural properties, the surface area of bulk and supported acid samples determined from N₂ adsorption–desorption isotherms using BET and BJH methods, together with the *t*-plot micropore area, BET adsorption average pore width, BJH adsorption average pore width and the *t*-plot micropore volume, are shown in Table 1. All properties of bulk HPA are lower, in all cases the values are close to the experimental error of the methods used. This is in agreement with previously reported information [48], although the bulk acids show negative adsorption data, attributed to a partial reduction of the acids due to the highly hygroscopic nature of the solid, causing an electronic delocalization that repulses the nitrogen molecules, generating gas desorption. In addition, according to the surface microvalues calculated using the *t*-plot method (Table 1), more than 70% of the total surface area comes from a mesoporous structure.

Finally, in Fig. 5, SEM micrographs of PWMoSiO₂ are shown, together with superficial analysis (mapping) of Si, Mo and W, respectively. The morphological aspect of all synthesized samples is similar, and the distribution of Mo/W atoms in the solid is homogeneous.

3.2. Catalytic test

Optimum reaction conditions were examined employing cinnamic acids and phthalimido ethanol as test reaction substrates. Initially, silica gel was used as catalyst in refluxing toluene and no reaction was observed (Table 2, entry 1). Then Preyssler acids and salts were tested (Table 2, entries 3–4, 6–7), and the results are interesting to analyze. The K salts, in both cases, do not yield any product; perhaps the intrinsic acid of Preyssler structure salt is not strong enough to produce phthalimidoethyl cinnamate. When PW and PWMo are used as catalysts, the yields are 62 and 66, for an initial *E* of 862 and 833 mV, respectively, this behavior confirming that the strong acid sites drive the reaction. Finally, when supported catalysts are used (Table 2, entries 5 and 8), PWMoSiO₂ is the most suitable catalyst. The reuse of this acid was tested under the same conditions, showing a small decrease of the yield (Table 2, entry 8b).

In order to obtain the optimal temperature, three temperatures (20, 80 and 110 °C, Table 3) were tested, using PWMoSiO₂ (1 mol%) under toluene as solvent, for different reaction times. At 20 °C, the reaction systems do not yield any reaction product at 7, 14 and 24 h. When the reaction temperature is increased to 80 °C, for the same reaction times, the yield increases to 58% for 24 h. The toluene boiling point (110 °C) was then tested under the same reaction conditions. The increase of the yields with temperature and reaction time was consistent (Table 3, entry 9). It is important to say that the PWMo acid is insoluble in a reaction medium because toluene is a nonpolar solvent. For this reason when PWMo is supported on silica, it is not soluble in the solvent although the temperature used was very high for the HPA. In order to evaluate

Table 1
Textural properties of catalysts.

Catalyst	BET surface area (m ² /g)	<i>t</i> -Plot micropore area (m ² /g)	BET adsorption average pore width (Å)	BJH adsorption average pore width (Å)	<i>t</i> -Plot micropore volume (m ³ /g)
PW	0.81	0.23	93.11	295.6	0.00
PMo	1.12	0.07	95.81	223.76	0.00
PWSiO ₂	239.74	28.92	166.86	164.45	0.01
PWMoSiO ₂	227.28	27.09	172.18	169.92	0.01

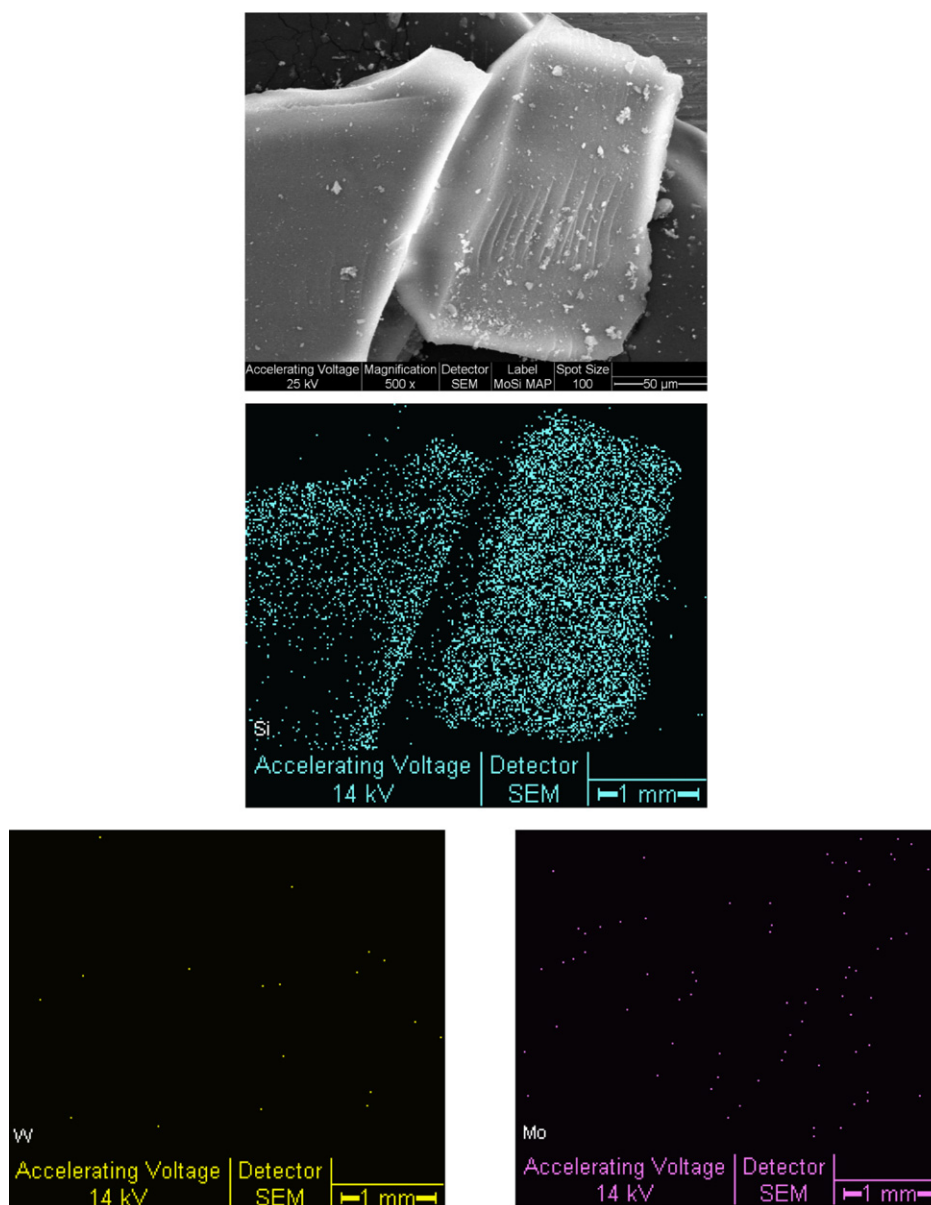


Fig. 5. SEM micrographs of PWMoSiO₂ and mapping on the same sample of Si, W and Mo.

the possible catalyst solubilization, an additional test was performed. A PWMoSiO₂ sample was refluxed in toluene for 2 h, filtered and dried in vacuum till constant weight. The activity of the so-treated catalyst was the same as that of the fresh catalyst (81% in 24 h). The refluxed toluene was used as solvent for attempting

the reaction without adding the catalyst. After 24 h cinnamate was not detected and the starting material was quantitatively recovered.

In relation to the catalyst amount, the results (Table 4) show 1 mol% concentration as the optimal quantity (Table 4, entry 3). In

Table 2

Esterification of cinnamic acid with 2-(N-phthalimido)ethanol using various Preyssler heteropolyacid catalysts^a.

Entry	Catalyst	Yields (%)
1	None	0
2	Silica (support)	0
3	PWK	0
4	PW	62
5	PWSiO ₂	75
6	PWMoK	0
7	PWMo	66
8	PWMoSiO ₂	82 (76) ^b

^a Reaction conditions: 1 mmol cinnamic acid, 1 mmol 2-(N-phthalimido)ethanol, 4 ml of toluene, 1 mmol% catalyst, 110 °C, stir, 24 h.

^b Reuse.

Table 3

Temperature optimization for the synthesis of 2-phthalimidoethyl cinnamate^a using PWMoSiO₂ as catalyst.

Entry	Temperature (°C)	Time (h)	Yields (%)
1	20	7	0
2	20	14	0
3	20	24	0
4	80	7	42
5	80	14	49
6	80	24	58
7	110	7	43
8	110	14	58
9	110	24	82

^a Reaction conditions: Cinnamic acid (1 mmol), 2-(N-phthalimido)ethanol (1 mmol) and PWMoSiO₂ (1 mol%) at different temperatures under toluene.

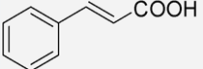
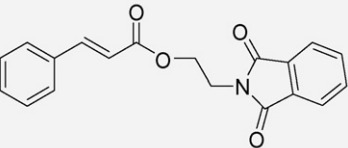
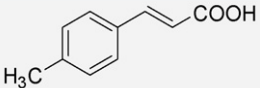
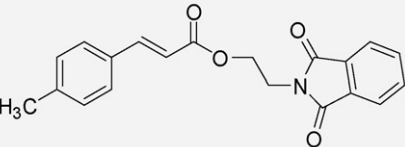
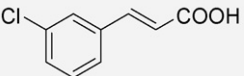
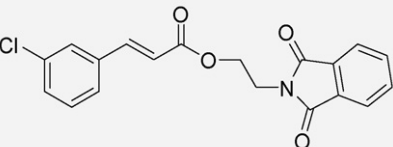
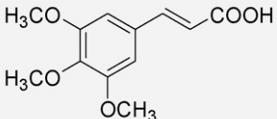
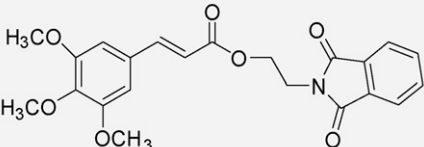
Entry	Catalyst concentration (mol%)	Yields (%)
1	0.1	26
2	0.5	55
3	1	82
4	2	83

this case it is possible to observe that the yield is directly proportional to the amount of catalyst used. The acid strength of PWMoSiO_2 is high but the number of acid sites is low, so it is necessary to increase the amount of active phase.

For phenol esterification, the subject reaction was performed using cinnamic acid and phenol as substrate. The test for the optimal catalyst gives the better results using again PWMoSiO₂ in a 7 h time period (Table 6, entry 5). The reuse assays give no changes after the catalyst reuse under the same conditions (Table 6, entry 6).

The influence of water was tested by reproducing the optimal reaction conditions for cinnamic acid esterification with phenol (Table 6) in the presence of molecular sieves (3 Å). The resulting 91% yield (Table 6, entry 6) shows no significant difference, suggesting low influence of water on the reaction.

In this case, the solvent volume is a relevant aspect, because 5% of subproduct 4-phenyl-3,4-dihydrocoumarin was observed when a low volume (1 ml) was used. In fact, this is the main selective product in the case of solvent-free reaction conditions from the same substrates [49] (Scheme 2). The lowering of reaction time when phenol was used replacing phthalimidoethanol can be attributed to an interaction of the oxygen atoms of the imido group with the acid catalyst (Scheme 3); this fact is supported by evidence of the decrease in the yield after reuse (Table 2, entry 8), probably due to the catalyst-imidoalcohol interaction.

Entry	Cinnamic acid	Product	Yields (%)
1			82
2			84
3			27
4			62

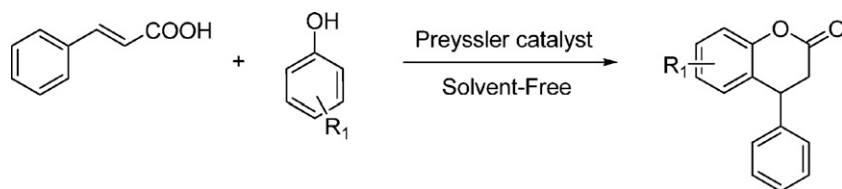
^a Reaction conditions: cinnamic acids (1 mmol) and 2-(N-phthalimido)ethanol (1 mmol). PWMoSiO₂ (1 mol%) at 110 °C, toluene, 24 h stirring.

Entry	Catalyst	Time (h)	Yields (%)
1	None	7	–
2	Silica (support)	7	–
3	PWMo	4	39
4	PWMoSiO ₂	4	49
5	PWMoSiO ₂	7	87
6	PWMoSiO ₂	14	89 (86) ^b ; (91) ^c

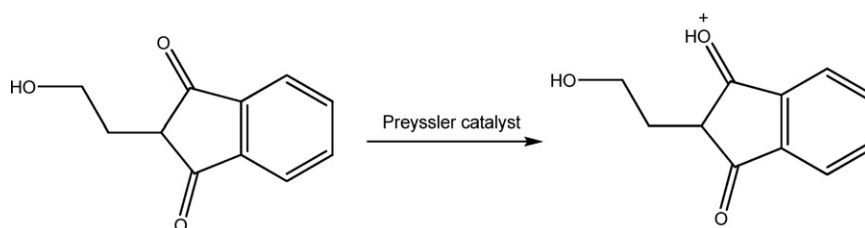
^a Reaction conditions: 1 mmol cinnamic acid, 1 mmol phenol, 4 ml of toluene, 1 mmol% catalyst, 110°C, stirring.

^b Reuse.

^c Using molecular sieves (3 Å).



Scheme 2.



Scheme 3.

Again, with the optimal conditions defined (PWSiO₂ 1 mmol% as catalyst, 7 h in refluxing toluene), substituted arylcinnamates were prepared from substituted cinnamic acids (Table 7). No changes were observed with different electronic substitutions of phenol.

As a result of the assays performed and informed in this research, in Fig. 6 we propose a catalytic cycle for the esterification of cinnamic acids with phenols using PWMo as

catalyst. The cycle begins with the protonation of the carboxylic oxygen of the cinnamic acid caused by the HPA; this interaction generates a carbocation in the carboxylic carbon atom that is later attacked by a phenol molecule acting as nucleophile. The instability of the generated ion promotes the proton transfer and consequent water molecule elimination, generating a new cation that finally deprotonates, giving the aryl cinnamate and recovering the catalyst.

Table 7

Synthesis of different phenyl cinnamates using PWMoSiO₂ as catalyst^a.

Entry	Phenol	Products	Yields(%)
1			87
2			89
3			85
4			86
5			78
6			95

^a Reaction conditions: cinnamic acid (1 mmol) and phenols (1 mmol). PWMoSiO₂ (1 mol%) at 110 °C, toluene, 7 h stirring.

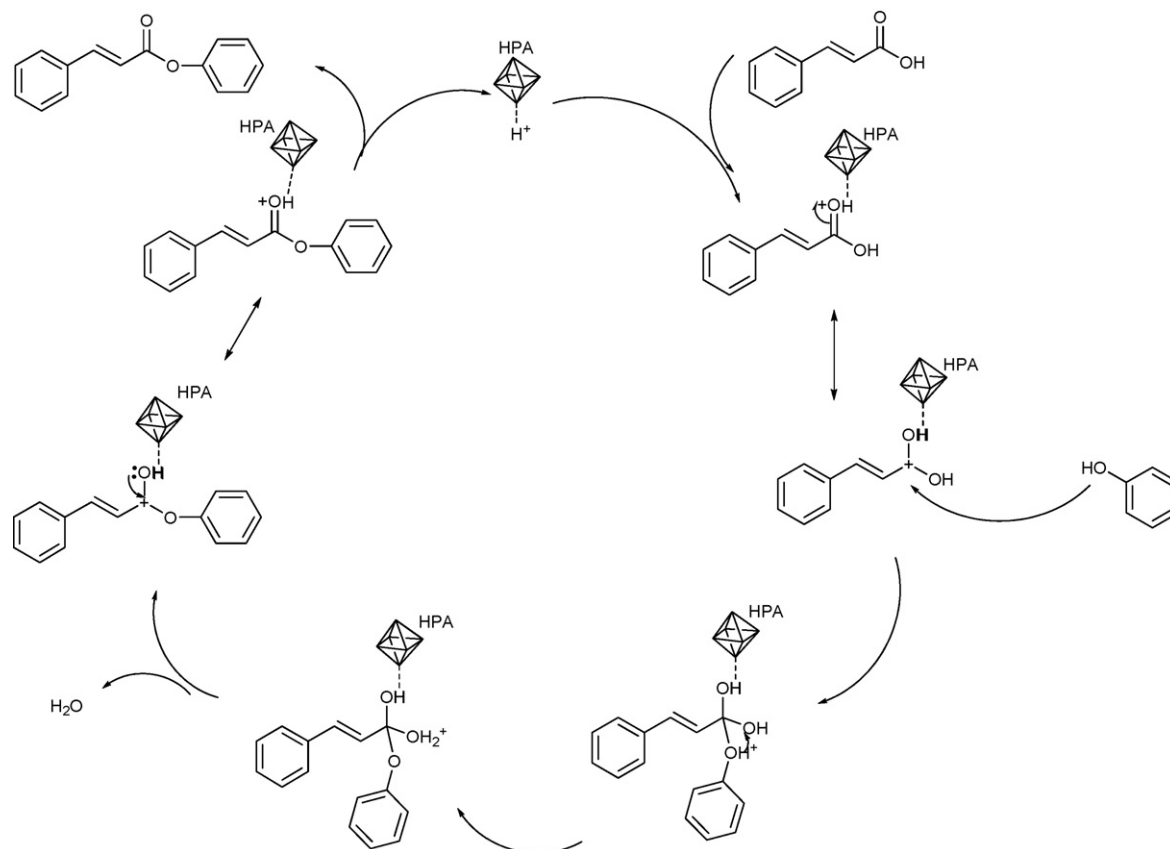


Fig. 6. Proposed catalytic cycle for the aryl cinnamate Preyssler acid-mediated esterification.

4. Conclusions

The described procedure for direct esterification using a mixed addenda Preyssler HPA $H_{14}[NaP_5W_{29}MoO_{110}]$ results in a clean and useful alternative for the preparation of aryl and phthalimidoethyl cinnamates; the advantages of this methodology are operative simplicity, use of a reusable and noncorrosive solid acid catalyst, soft reaction conditions, and good yields.

The use of a solid acid catalyst instead of the usual soluble acid catalyst (sulfuric, hydrochloric, etc.) contributes to a reduction in waste generation by allowing an easy separation and recovery without any loss of its catalytic activity.

Acknowledgements

We thank Agencia Nacional de Promoción Científica y Tecnológica (Argentina), Fundación Antorchas, Universidad Nacional de La Plata, and CONICET for financial support.

References

- [1] M. Misono, N. Nojiri, *Appl. Catal. A: Gen.* 64 (1990) 1–30.
- [2] T. Okuhara, *Catal. Today* 73 (2002) 167–176.
- [3] N. Mizuno, M. Misono, *Chem. Rev.* 98 (1998) 199–217.
- [4] I. Kozhevnikov, *Chem. Rev.* 98 (1998) 171–198.
- [5] G. Yadav, *Catal. Surv. Asia* 9 (2005) 117–137.
- [6] I. Kozhevnikov, *J. Mol. Catal. A: Chem.* 262 (2007) 86–92.
- [7] M. Yarmo, R. Shariff, S. Omar, J. Ching, R. Haron, *Mater. Sci. Forum* 517 (2006) 117–122.
- [8] M. Misono, I. Ono, G. Koyano, G. Aoshima, *Pure Appl. Chem.* 72 (2002) 1305–1311.
- [9] M. Heravi, S. Sadjadi, *J. Iran Chem. Soc.* 6 (2009) 1–54.
- [10] N. Mizuno, M. Misono, *Curr. Opin. Solid State Mater. Sci.* 2 (1997) 84–89.
- [11] L. Pizzio, P. Vázquez, C. Cáceres, M. Blanco, *Appl. Catal. A: Gen.* 256 (2003) 125–139.
- [12] P. Vázquez, L. Pizzio, G. Romanelli, J. Autino, C. Cáceres, M. Blanco, *Appl. Catal. A: Gen.* 235 (2002) 233–240.
- [13] M. Heravi, M. Khorasani, F. Derikvand, H. Oskooie, F. Bamoharram, *Catal. Commun.* 8 (2007) 1886–1890.
- [14] I. Kozhevnikov, *Catal. Rev. Sci. Eng.* 37 (1995) 311–352.
- [15] M. Pope, *Heteropoly and Isopoly Oxometalates*, Springer, Berlin, 1983.
- [16] L. Briand, G. Baronetti, H. Thomas, *Appl. Catal. A: Gen.* 256 (2003) 37–50.
- [17] F. Bamoharram, M. Heravi, M. Roshani, M. Jahagiri, A. Gharib, *Appl. Catal. A: Gen.* 302 (2006) 42–47.
- [18] S. Wu, J. Wang, W. Zhang, X. Ren, *Catal. Lett.* 125 (2008) 308–314.
- [19] R. Hekmatshoar, M. Heravi, S. Sadjadi, H. Oskooie, F. Bamoharram, *Catal. Commun.* 9 (2008) 837–841.
- [20] M. Heravi, F. Derikvand, A. Haeri, H. Oskooie, F. Bamoharram, *Synth. Commun.* 38 (2008) 135–140.
- [21] M. Heravi, K. Bakhtiari, Z. Daroogheha, F. Bamoharram, *Catal. Commun.* 8 (2007) 1991–1994.
- [22] M. Heravi, K. Bakhtiari, V. Zadsirjan, F. Bamoharram, O. Heravi, *Bioorg. Med. Chem. Lett.* 17 (2007) 4262–4265.
- [23] M. Heravi, F. Derikvand, L. Ranjbar, F. Bamoharram, *J. Mol. Catal. A: Chem.* 261 (2007) 156–159.
- [24] M. Heravi, V. Zadsirjan, K. Bakhtiari, H. Oskooie, F. Bamoharram, *Catal. Commun.* 8 (2007) 315–318.
- [25] F. Bamoharram, H. Heravi, M. Roshani, A. Akbarpour, *J. Mol. Catal. A Chem.* 255 (2006) 193–198.
- [26] R. Hekmatshoar, S. Sajadi, M. Heravi, F. Bamoharram, *Molecules* 12 (2007) 2223–2228.
- [27] A. Kharat, M. Amini, M. Abedini, *React. Kinet. Catal. Lett.* 84 (2005) 37–43.
- [28] M. Petersen, M. Simmonds, *Phytochemistry* 62 (2003) 121–125.
- [29] A. Sinha, A. Sharma, A. Swaroop, V. Kumar, *Tetrahedron* 63 (2007) 1000–1007 (And references cited herein).
- [30] S. Gobec, M. Sova, K. Kristan, T. Rizner, *Bioorg. Med. Chem. Lett.* 14 (2004) 3933–3936.
- [31] C. Pinto, A. Silva, A. Cavaleiro, J. Foces-Foces, A. Llamas-Saiz, N. Jegerovic, *Tetrahedron* 55 (1999) 10187–10200.
- [32] J. Zhu, M. Majikina, S. Tawata, *Biosci. Biotechnol. Biochem.* 65 (2001) 161–163.
- [33] E. Womack, J. McWhirter, *Org. Synth. Coll. III* (1955) 714–715.
- [34] N. Isaacs, T. Najem, *J. Chem. Soc. Perkin Trans. 2* (1988) 557–562.
- [35] R. Mali, A. Papalkar, *J. Chem. Res. (S)* (2003) 603–605 (And references cited therein).
- [36] D. Ruiz, G. Romanelli, D. Bennardi, G. Baronetti, H. Thomas, J. Autino, *Arkivoc* vii (2008) 269–276.

- [37] M. Nakayama, A. Sato, K. Ishihara, H. Yamamoto, *Adv. Synth. Catal.* 346 (2004) 1275–1279.
- [38] I. Creaser, M. Heckel, R. Neitz, M. Pope, *Inorg. Chem.* 32 (1993) 1573–1578.
- [39] M. Arabi, M. Amini, M. Abedini, A. Nemati, A. Alizadeh, *J. Mol. Catal. A: Chem.* 200 (2003) 105–110.
- [40] M. Sova, A. Perdih, M. Kotnik, K. Kristan, T.L. Rižner, T. Solmajer, S. Gobec, *Bioorg. Med. Chem.* 14 (2006) 7404–7418.
- [41] H. Obara, H. Takahashi, J. Onodera, *Kogyo Kagaku Zasshi* 72 (1969) 309–310.
- [42] T. Fife, T. Przystas, M. Pujari, *J. Am. Chem. Soc.* 110 (1988) 8157–8163.
- [43] S. Hashimoto, I. Furukawa, *Bull. Chem. Soc. Jpn.* 54 (1981) 2227–2228.
- [44] J. Gerig, R. McLeod, *Can. J. Chem.* 53 (1975) 513–514.
- [45] P. Villabrille, G. Romanelli, P. Vázquez, C. Cáceres, *Appl. Catal. A: Gen.* 270 (2004) 101–111.
- [46] G. Romanelli, P. Vázquez, L. Pizzio, N. Quaranta, J. Autino, M. Blanco, C. Cáceres, *Appl. Catal. A: Gen.* 261 (2004) 163–170.
- [47] S. Jiang, Y. Guo, C. Wang, X. Qu, L. Li, *J. Colloid Interface Sci.* 308 (2007) 208–215.
- [48] A. Kharat, M. Abedini, M. Amini, P. Pendleton, A. Badalyan, *Transition Metal Chem.* 28 (2003) 339–344.
- [49] D. Bennardi, D. Ruiz, G. Romanelli, G. Baronetti, H. Thomas, J. Autino, *Lett. Org. Chem.* 5 (2008) 607–615.